Effect of Antifreeze Protein on Nucleation, Growth and Memory of Gas Hydrates

Huang Zeng, Igor L. Moudrakovski, and John A. Ripmeester
Steacie Institute for Molecular Sciences, National Research Council of Canada, Ottawa, ON K1A 0R6, Canada

Virginia K. Walker
Dept. of Biology, Queen's University, Kingston, ON K7L 3N6, Canada

DOI 10.1002/aic.10929
Published online June 29, 2006 in Wiley InterScience (www.interscience.wiley.com).

The effect of Type I antifreeze protein (AFP) from winter flounder on the formation of propane hydrate and methane hydrate was studied. We show that the formation of both hydrates is inhibited significantly, with both nucleation and crystal growth being affected. Also, AFP showed the so-far unique ability to eliminate the "memory effect" in the reformation of gas hydrate. We have proposed a mechanism involving the interference of AFP with heterogeneous nucleation and subsequent growth of the hydrates. It is also shown that a number of samples must be studied in order to obtain meaningful statistics, and that magnetic resonance imaging provides a novel way of studying the nucleation and growth of hydrate in multiple droplets. © 2006 American Institute of Chemical Engineers
AIChE J, 52: 3304–3309, 2006
Keywords: inhibition, hydrocarbon hydrate, antifreeze protein, NMR microscopy

Introduction

The formation of gas hydrates during hydrocarbon production and transportation is a serious problem in the petroleum industry.[1] To prevent the formation of gas hydrate, chemicals such as methanol have been widely used as a thermodynamic inhibitor, despite concerns about methanol's environmental effects as well as the expense due to the large amounts required.[2] During the past decade, some new "low dosage hydrate inhibitors" (LDHIs) have drawn much attention because of their ability to either retard the formation of gas hydrate (kinetic inhibitors, KIs) or to prevent the aggregation of small hydrate crystals (anti-agglomerants, AAs).[3] Despite the fact that the development of LDHIs was inspired by the discovery of antifreeze glycoprotein (AFGP),[4] antifreeze proteins (AFP) and AFGP have not been studied for hydrate inhibition nearly as much as synthetic LDHIs, probably because of the limited availability of these materials. Recently, hyperactive AFPs have been found in insects and polar fish,[5,6] and progress has been made in the understanding of the structure and function of several AFPs.[7,8] Therefore, it is worthwhile to study the potential inhibition activities of AFPs to gas hydrate formation in order to design new LDHIs with higher inhibition activities.

Previous experiments have shown that commercial gas hydrate inhibitors, such as polyvinylpyrrolidone (PVP), inhibit the formation of a structure II tetrahydrofuran (THF), often used as a model system.[9,10] We have shown that Type I AFP from winter flounder surpasses PVP's inhibition activity of THF hydrate.[10] Although the model for the inhibition of THF hydrate likely is valid, there are some differences between this hydrate and natural gas hydrates. First, without agitation, the formation of gas hydrates usually starts from the water/hydrocarbon interface,[11] making the behavior of the inhibitor molecules at the interface an important issue; whereas THF hydrate forms within a single aqueous phase. Second, it is possible that the high concentration of THF (~20 wt%) in the model hydrate solution could affect the properties of inhibitor molecules in a way that would not happen for actual hydrocarbon gas hydrate-forming systems. Therefore, it is important to determine if AFPs can also inhibit hydrocarbon gas hydrates, as these do

Correspondence concerning this article should be addressed to J. A. Ripmeester at john.ripmeester@nrc-cnrc.gc.ca.

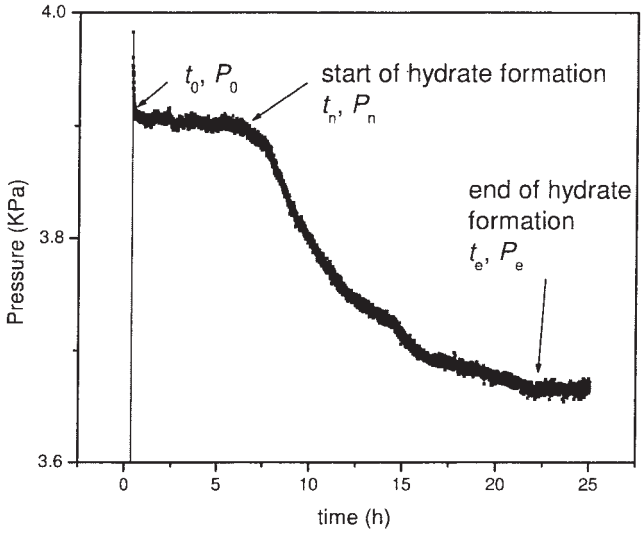

Figure 1. A typical gas uptake curve observed during propane hydrate formation.

cause very real problems in gas pipelines and drilling operations.

Experimental

Purified Type I fish AFP from the winter flounder (wfAFP) was kindly provided by A/F Protein Canada Inc. This, the most extensively studied Type I AFP, is comprised of 37 amino acids and contains three 11 amino acid repeats of Thr-X_2-Asx-X_7 where X is generally Ala. The protein is a monomeric α-helix,[12] with its helicity preserved by the high Ala content (>60%), internal salt bridges, and N- and C-terminal cap structure.[13] Water of HPLC grade was used in this study.

For propane hydrate formation experiments, wfAFP was prepared as a 0.25 mM aqueous solution. Test solutions (water or AFP solution) of 5 ml were sealed in a high-pressure cell (~30 ml) at 278 K and degassed under vacuum (using a water pump) for 1 h. Propane gas (99.99%) at ~400 KPa was then introduced into the cell. Subsequently, the temperature of the cell was decreased to 273 K while stirring the solution with a magnetic stir bar. The pressure of the gas and temperature of the solution were recorded, and a sudden drop in pressure was noted as the onset of gas hydrate formation (Figure 1). Five independent samples were tested for each test solution.

To test the effect of AFP on hydrate reformation, the propane hydrate that crystallized either in the presence or absence of additives in the test solution was kept completely frozen at 194.5 K for 0.5 h by placing the high-pressure cell in dry ice. The cell was then transferred into a bath at 275 K for melting, and propane was removed from the cell under vacuum (using the water pump) at the same time, all the while stirring, for 1 h. The temperature of the bath was then lowered to 273 K and, when the temperature of the test solution in the cell reached equilibrium, propane gas (~400 KPa) was re-introduced and the recording started to monitor the second round of hydrate formation.

For the ^{1}H NMR microimaging experiments, 0.25 mM wfAFP aqueous solution (containing 25 mM $Cu(NO_3)\cdot 2.5H_2O$) was prepared (copper nitrate was added to reduce the relaxation time of the protons and, therefore, to reduce data acquisition times for the NMR imaging). Although it is well-known that electrolyte solutions can inhibit the formation of gas hydrate, the concentration of the electrolyte used in this experiment is so low (mM) that it should not affect the formation of methane hydrate in this study.

The diagram of the sample tube for imaging (I) and the insert for ^{1}H NMR micro-imaging (II) of water droplets is shown in Figure 2b. The imaging tube and insert were made from Torlon® (polyamide-imide (PAI), from Boedeker Plastics, Texas). It includes a base with a supporting rod, and three stackable rounds, each of which has four holes (∅ 1 mm). In each experiment, water droplets (∅ 1 mm) were placed into the holes in the insert with a micro-syringe and transferred into the imaging tube. The samples were first degassed at −69 KPa for 1min, then pressurized with methane gas at 11.7 MPa at 274.0K.

The ^{1}H NMR microimaging experiments were performed on a Bruker Avance200 NMR instrument using a multi-slice spin-echo pulse sequence with Gaussian selective pulses (slice, read, and phase gradients were 43, 35, and 71 G/cm, respectively). Normally, three slices 500 μm thick with a separation of 1.5 mm (shown as dashed-line box) were acquired simultaneously in a plane parallel to the axis of the cell, as shown in Figure 2b. A 192 × 192 acquisition matrix was extended to 256 × 256 for Fourier-transformation. In the experiments, 8 scans were accumulated in order to obtain a good signal-to-noise ratio (pixel size 0.1 mm).

Results and Discussion

For the propane hydrate formation experiments, hydrate formation was monitored by gas uptake, and a sudden drop in pressure marked the start of hydrate formation (Figure 1). The time between the point at which the pressure drop started and the point at which the solution reached equilibrium pressure ($t_n - t_0$) was recorded as the induction time (t_i). From Figure 1, it can be seen that the gas consumption rate changed with time, consistent with the fact that the driving force of hydrate formation is time-dependent. To simplify the calculation, the average gas consumption rate (r) was calculated as

$$r = \frac{P_n - P_e}{t_e - t_n}$$

where P_e represents the pressure at the conclusion of the experiment, P_n is the pressure when hydrate nucleation is initiated (indicated by a drop in pressure), t_e is the time when the pressure reached equilibrium, and t_n is the time when the pressure dropped significantly (Figure 1).

The fraction of hydrate-free samples (N_t/N_0, where N_t is the number of hydrate-free samples at time t and N_0 is the number of hydrate-free samples at time 0) was plotted versus time for each test solution (Figure 3a). Assuming that the phase change in the test solution is a one-step transformation,[14] the nucleation rate, k, and the average lag time, τ, can be derived according to

$N_t/N_0 = \exp[-k\,t]$

and $\tau = k^{-1}$.

The results are listed in Table 1. The average gas consump-

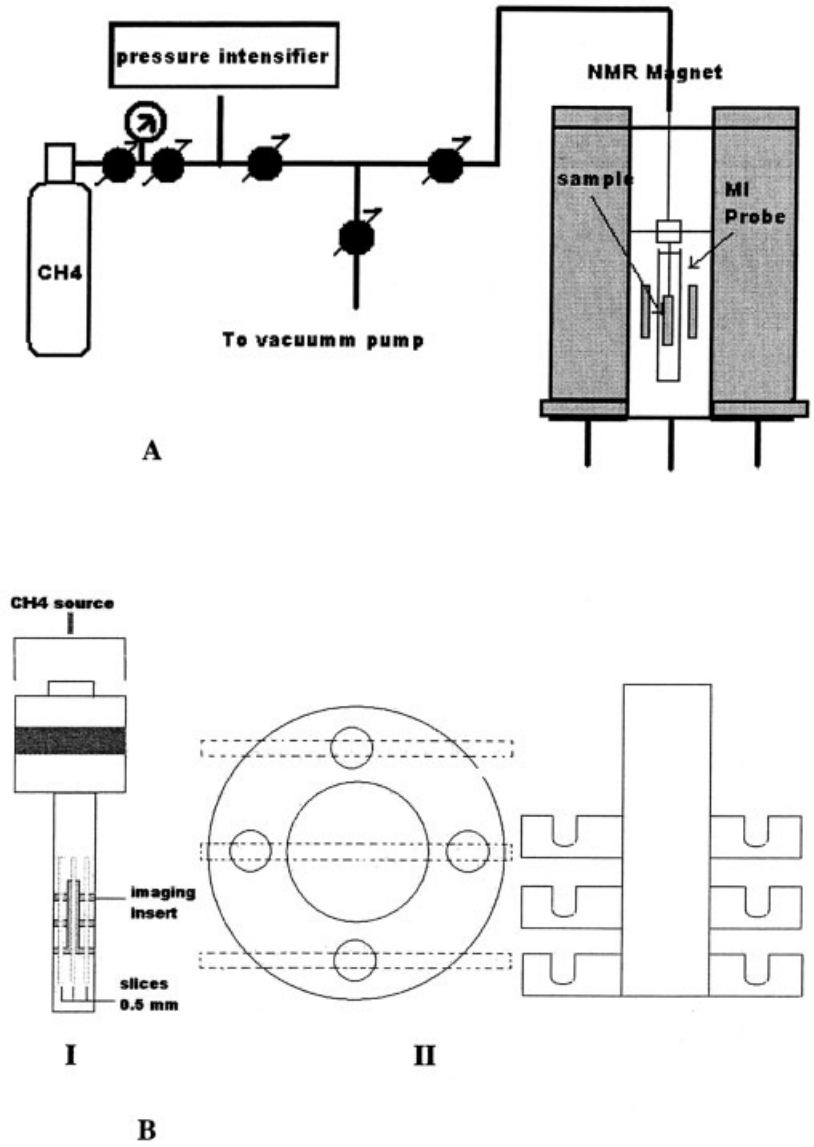

Figure 2. (a) The experimental apparatus for ^{1}H NMR microimaging, and (b) the high pressure cell (I) as well as the location of the positions of the three optical slices (II).

tion rate for propane hydrate formation from the test solutions was monitored (Figure 3b) and the data shown in Table 1. The addition of 0.25 mM AFP increased the lag time for nucleation 3-fold (56 versus 179 min) and reduced the hydrate growth rate in terms of the rate of gas consumption, r, 5-fold (4.1 versus 0.8 kPa/h), compared to propane hydrate reformation without AFP (Table 1).

Once hydrate forms and is melted, subsequently it reforms more easily.[15-18] This "memory effect" was observed when samples containing the melted propane hydrate were subjected to conditions again favoring hydrate formation; there was a 3-fold increase (18 versus 59×10^{-3} min^{-1}) in the nucleation rate for propane hydrate reformation. A memory effect was not observed in the presence of AFP since the nucleation rate was the same for both the formation and reformation of propane hydrate (5.6 versus 5.9×10^{-3} min^{-1}) within experimental error. Although it is expected that such a small volume of propane hydrate (5 ml) would be completely decomposed after being kept under vacuum at 275 K for 1 h while stirring, even if there is a very small concentration of propane hydrate remaining in the sample, it would not change the conclusion that the memory effect was "eliminated" by the presence of AFP since the difference is so significant. Notably, although the overall hydrate growth rate, as monitored by propane consumption, was lower in the presence of AFP, it did not appear to change from the first formation to the second in either AFP or control samples (Figure 3b and Table 1). Previously, we reported that AFPs were effective inhibitors of THF hydrate.[10] Here we show that wfAFP inhibits structure II propane hydrate formation, validating the utility of the model and confirming the inhibition activity of the protein, as demonstrated by the 3-fold increase in nucleation time and the 5-fold reduction in propane consumption (Figure 3 and Table 1). This inhibition, coupled with the remarkable suppression of the memory effect

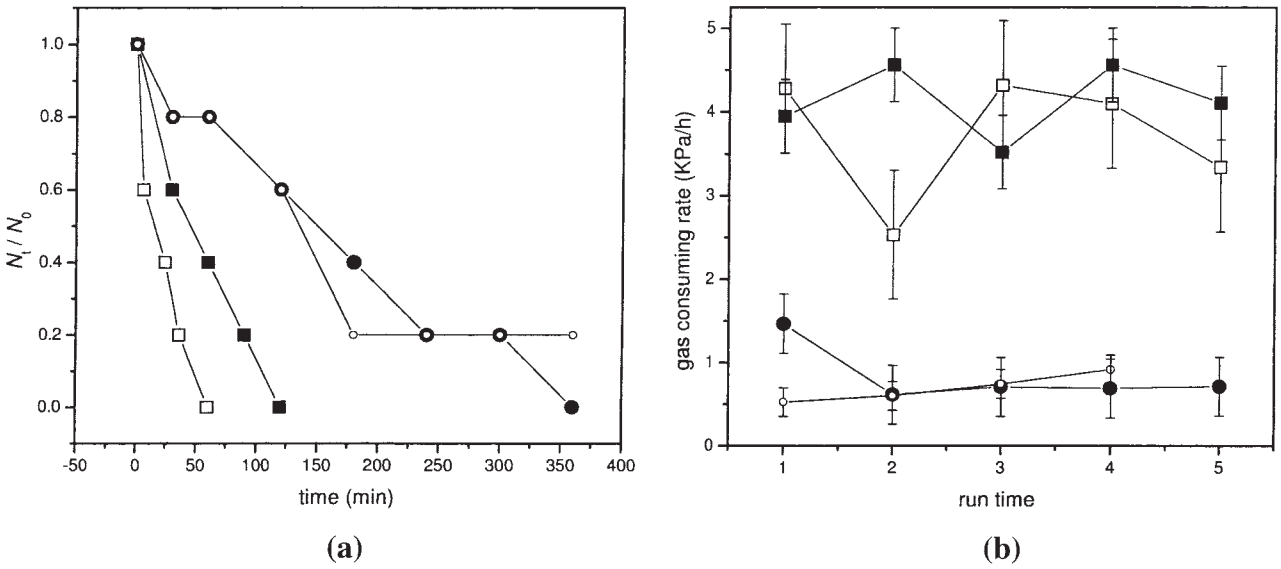

Figure 3. Inhibition of propane hydrate formation with AFP.

(a) The fraction of untransformed samples versus time for propane hydrate formed at 273 K, 400 Kpa, in the presence of water (■) and propane hydrate in the presence of 0.25 mM AFP (●). The hydrate was then melted and reformed, again in the presence of water (□) or AFP solution (○). N_t: number of unfrozen sample at time t; N_0: number of unfrozen sample at time 0. (b) Gas consumption rate of propane hydrate formed initially and reformed after melting. Samples were formed initially with water (■) and reformed after melting (□), or formed initially in the presence of 0.25 mM wfAFP (●) and reformed after melting (○). It should be noted that there was no transformation for run 5 for the reformation of hydrate in the presence of wfAFP. See Figure 3A.

of propane hydrate, indicates that AFPs are extraordinary hydrate formation inhibitors.

The NMR microimaging results for methane hydrate formed in the absence of AFP (Figure 4a) and for methane hydrate formed in the presence of AFP (Figure 4b) are presented as a series of three slices through water droplets at the positions shown in Figure 2b. Hydrate formation was recorded at the start of the experiment (time = 0, t_0) and at different times (t_a) after that. The formation of methane hydrate was followed quantitatively by monitoring the reduction in the amount of liquid phase present by measuring the change in liquid proton spin density in the NMR images. Visually, this becomes evident by a shrinking and a loss of intensity of the bright areas in the drop images as the amount of solid methane hydrate increases in each pixel (size 0.1 mm) The difference images (image at time $t = t_a - t_0$) present hydrate formation that occurs as a function of time, with the hydrate shown in black. The average conversion ratio calculated by comparing the intensity change of 9-10 droplet samples was more than 50% after 42 h (Figure 4c) for methane hydrate formed in water droplets in the absence of AFP. With wfAFP, the average conversion ratio was only 23% after 64 h, showing the strong inhibition activity of wfAFP to methane hydrate formation. Therefore, the average conversion rate of the test solution into methane hydrate decreased about 3-fold in the presence of AFP.

Table 1. Nucleation Rate (k), Average Lag Time (τ), and Rate of Gas Consumption (r) for Propane Hydrate

Hydrate Conditions	k ($\times 10^{-3}$ min^{-1})	τ (min)	r (KPa/h)
C_3H_8	17.9 ± 0.2	55.9 ± 0.6	4.1 ± 0.4
melted	58.8 ± 1.2	17.0 ± 0.4	3.7 ± 0.8
C_3H_8-wfAFP (0.25 mM)	5.6 ± 0.1	178.6 ± 2.7	0.8 ± 0.4
melted	5.9 ± 0.1	169.5 ± 2.9	0.7 ± 0.2

Means + standard deviation are shown for 5 experiments using propane hydrate (C_3H_8; at 273K, starting pressure is ~400 KPa) alone, or with wfAFP. The memory effect is shown by the difference (k, τ, and r) prior to and after melting.

The ^{1}H NMR imaging results presented here not only demonstrate that the technique has potential for the evaluation of hydrate formation and inhibition, but show that wfAFP indeed inhibits structure I methane hydrate formation (Figure 4). The addition of AFP reduced the conversion ratio of aqueous solutions to methane hydrate 3-fold. The inhibition of both propane and methane shows that AFP is effective for the inhibition of clathrate hydrate formation with different hydrate structures.

It has been documented that AFPs inhibit the formation of ice. A surface adsorption mechanism has been proposed, where, once protein molecules bind to the surface of ice, the growth of ice from the area between the adsorbed AFP molecules will be unfavorable. Growth in such a restricted area defined by AFP molecules "pinned" to the surface causes an increase in surface curvature, which then inhibits further growth (the Kelvin effect).[19]

One component of ice or hydrate inhibition that has received very little attention is that of nucleation. It has been demonstrated that AFPs control morphology and growth in ice and THF hydrate. Usually, gas consumption measurements are used to test the effectiveness of inhibitors. However, it is impossible to separate the effect of the inhibitors on the nucleation and growth processes that occur simultaneously in bulk solution. Separate indicators of nucleation and growth must be used. In some of our previous work on THF hydrate, we have shown that AFP in fact acts as an inhibitor of heterogeneous nucleation, that is, it takes place at sites provided by the container wall and impurity particles in bulk solution, and we

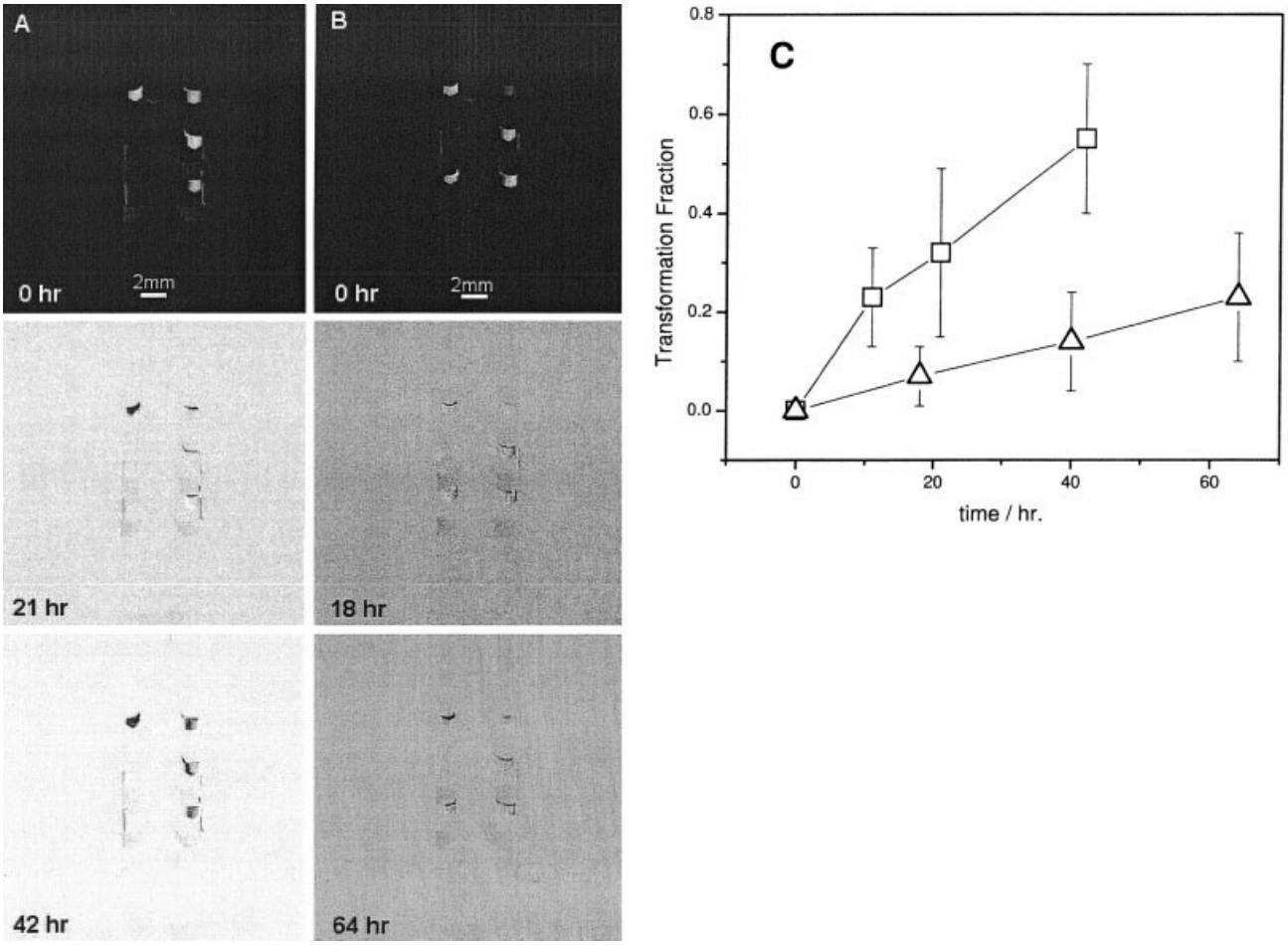

Figure 4. Representative ^{1}H NMR microimages of methane hydrate formation from water droplets in the absence of wfAFP (a) and in the presence of 0.25 mM wfAFP (b).

(The sample geometry is shown in Figure 2b). The average transformation rate to methane hydrate, obtained by integrating the proton spin density in each drop (indicated visually by the brightness in the drop images), is shown in c, both in the absence of wfAFP (□) and in the presence of 0.25 mM wfAFP(△).

have discussed the inhibition of hydrate formation and the memory effect with AFPs[20] in terms of an impurity mechanism. We can only speculate on the nature of impurities that may act as hydrate nucleators in bulk solution. Hydrated oxides (for instance, those of Si or Fe) are common contaminants of water, and such impurities are likely to have highly hydrated surfaces.

We can offer some further discussion on ice and hydrate inhibition-using AFPs that may be relevant in further elucidating the inhibition mechanism. It has been reported that an AFP analogue can bind to the surface of calcite.[21] The effect of AFP on the growth morphology of THF hydrate crystal[10] revealed that AFP adsorbs on the surface of a model gas hydrate. Our quartz crystal microbalance (QCM) experiments have also shown that AFPs adsorb on hydrophilic silica, forming a compact film.[22] It is apparent that AFPs will adsorb on most if not all hydrophilic surfaces, which is not unexpected for large molecules such as proteins. Previous work has suggested that ice has crystal faces on which AFPs adsorb preferentially, but that does not preclude the adsorption of AFPs on any suitable hydrophilic surface, such as hydrate crystals of several structures, calcite, and amorphous silica. The QCM measurements on amorphous silica suggest that the rapid formation of a rigid film on hydrophilic surfaces is a key element of the inhibition activities, as this ability distinguishes AFPs from synthetic inhibitors. AFP film formation, therefore, should take place both on hydrate crystals and on hydrophilic impurities and, therefore, heterogeneous nucleation, growth, and the memory effect all can be affected. In our studies it was shown that AFP can inhibit the faster reformation (that is, the memory effect) in propane hydrate as well as for THF hydrate.[20] To our knowledge, this is the first report of any molecule that can eliminate the memory effect in natural gas hydrate formation. We believe that applications of these results can have an important impact on the safe and economical transportation of natural gas and/or oil. The fact that the propane gas consumption rate did not change during the reformation of propane hydrate in the presence of AFP also confirms that the memory effect is more likely related to the nucleation stage of hydrate formation rather than the growth stage.

In summary, AFP inhibits the formation of not only the model hydrate, THF hydrate, but also natural gas hydrates of sI and sII, propane, and methane hydrates. In this work and in a study with THF hydrate,[22] this protein also shows the unique

ability to inhibit the memory effect. These favorable features and new insights make the study of AFP hydrate inhibitors crucially important for their potential utility for industry. More detailed studies, such as the structure-inhibition activity relationship of AFPs on gas hydrate formation, will give additional insights into the mechanism of action of the LDHIs and also will help in designing a new generation of LDHIs.

Acknowledgments

We thank A/F Protein Canada Inc. (Dr. G. Fletcher and Dr. S. Goddard) for providing the Type I AFP. The NSERC/NRC/Industry partnership program is acknowledged for a grant to Virginia K. Walker and John A. Ripmeester. Partial support for Huang Zeng was provided by a Queen's University graduate scholarship and a PetroCanada research scholarship.

Literature Cited

1. Mehta AP, Klomp UC. An industry perspective on the state of the art of hydrates management. *Proc 5th International Conference on Gas Hydrate.* 2005;4:1089-1100.
2. Koh CA, Westacott RE, Zhang W, Hirachand K, Creek JL, Soper AK. Mechanisms of gas hydrate formation and inhibition. *Fluid Phase Equil.* 2002;194:143-151.
3. Huo Z, Freer E, Lamar M, Sannigrahi B, Knauss DM, Sloan ED Jr. Hydrate plug prevention by anti-agglomeration. *Chem Eng Sci.* 2001; 56:4979-4991.
4. DeVries AL. Glycoproteins as biological antifreeze agents in antarctic fishes. *Science.* 1971;172:1153-1155.
5. Tyshenko MG, Doucet D, Davies PL, Walker VK. The antifreeze potential of the spruce budworm thermal hysteresis protein. *Nat Biotechnol.* 1997;15:887-890.
6. Marshall CB, Fletcher GL, Davies PL. Hyperactive antifreeze protein in a fish. *Nature.* 2004;429:153.
7. Yeh Y, Feeney RE. Antifreeze proteins: structures and mechanisms of function. *Chem Rev.* 1996;96:601-618.
8. Davies PL, Baardsnes J, Kuiper MJ, Walker VK. Structure and function of antifreeze proteins. *Philos Trans R Soc Lond B Biol Sci.* 2002;357:927-933.
9. Larsen R, Knight CA, Sloan ED Jr. Clathrate hydrate growth and inhibition. *Fluid Phase Equil.* 1998;150-151:353-360.
10. Zeng H, Wilson LD, Walker VK, Ripmeester JA. The inhibition of tetrahydrofuran clathrate hydrate formation with antifreeze protein. *Can J Phys.* 2003;81:17-24.
11. Makogon YF. *Hydrates of Hydrocarbons*. Tulsa, OK: Penn Well Publishing Company; 1997.
12. Gronwald W, Chao H, Reddy DV, Davies PL, Sykes BD, Sönnichen FD. The solution structure of type II antifreeze protein reveals a new member of the lectin family. *Biochem.* 1999;35:16698-16704.
13. Sicheri F, Yang DSC. Ice-binding structure and mechanism of an antifreeze protein from winter flounder. *Nature.* 1995;375:427-431.
14. Heneghan AF, Wilson PW, Wang G, Haymet ADJ. Liquid-to-crystal nucleation: automated lag-time apparatus to study supercooled liquids. *J Chem Phys.* 2001;115:7599-7608.
15. Takeya S, Hori A, Hondoh T, Uchida T. Freezing-memory effect of water on nucleation of CO_2 hydrate crystals. *J Phys Chem B.* 2000; 104:4164-4168.
16. Sloan ED Jr. *Clathrate Hydrates of Natural Gases* (2nd edition). New York: Marcel Dekker Inc.; 1998.
17. Servio P, Englezos P. Morphology of methane and carbon dioxide hydrates formed from water droplets. *AIChE J.* 2003;49(1):269-276.
18. Ohmura R, Ogawa M, Yasuoka K, Mori YH. Statistical study of clathrate-hydrate nucleation in a water/hydrochlorofluorocarbon system: search for the nature of the "memory effect." *J Phys Chem B.* 2003;107:5289-5293.
19. Knight CA. Adding to the antifreeze agenda. *Nature.* 2000;406:249-250.
20. Zeng H, Walker VK, Ripmeester JA. Examining the classification of low dosage hydrate inhibitors. *Proc 5th International Conference on Gas Hydrate.* 2005;4:1295-1299.
21. DeOliveira D, Laursen R. Control of calcite crystal morphology by a peptide designed to bind to a specific surface. *J Am Chem Soc.* 1997;109:10627-10631.
22. Zeng H. Ph.D. thesis, Queen's University, Canada, 2004.

Manuscript received Sept. 13, 2005, revision received Feb. 22, 2006, and final revision received May 25, 2006.